# Recombinant inbred line panels inform the genetic architecture and interactions of adaptive traits in *Drosophila melanogaster*

**Authors**: Tiago da Silva Ribeiro[1,2,a,@], Matthew J. Lollar[1], Quentin D. Sprengelmeyer[1b], Yuheng Huang[1c], Derek M. Benson[1], Megan S. Orr[1], Zachary C. Johnson[1], Russell B. Corbett-Detig[3,4], John E. Pool[1,2,@]

**Mailing address:**

[1] Laboratory of Genetics, University of Wisconsin-Madison, Madison, WI, 53706, USA

[2] Department of Integrative Biology, University of Wisconsin-Madison, Madison, WI, 53706, USA

[3] Genomics Institute, University of California, Santa Cruz, Santa Cruz, CA, 95064, USA

[4] Department of Biomolecular Engineering, University of California, Santa Cruz, Santa Cruz, CA, 95064, USA

[a] Current address: Instituto de Biociências, Universidade de São Paulo, São Paulo, Brazil, 05508-090.

[b] Current address: Department of Equity and Inclusion, University of Wisconsin-Platteville, Platteville, WI, 53818

[c] Current address: Department of Ecology and Evolutionary Biology, University of California, Irvine, Irvine, CA, 92697.

**[@] Corresponding authors:**

Tiago da Silva Ribeiro, tribeiro@wisc.edu

John E. Pool, jpool@wisc.edu

**Keywords**: epistasis, Quantitative Trait Loci (QTL), adaptation, quantitative genetics, *Drosophila melanogaster*.

## Abstract

The distribution of allelic effects on traits, along with their gene-by-gene and gene-by-environment interactions, contributes to the phenotypes available for selection and the trajectories of adaptive variants. Nonetheless, uncertainty persists regarding the effect sizes underlying adaptations and the importance of genetic interactions. Herein, we aimed to investigate the genetic architecture and the epistatic and environmental interactions involving loci that contribute to multiple adaptive traits using two new panels of *Drosophila melanogaster* recombinant inbred lines (RILs). To better fit our data, we re-implemented functions from R/qtl (Broman *et al.* 2003) using additive genetic models. We found 14 quantitative trait loci (QTL) underlying melanism, wing size, song pattern, and ethanol resistance. By combining our mapping results with population genetic statistics, we identified potential new genes related to these traits. None of the detected QTLs showed clear evidence of epistasis, and our power analysis indicated that we should have seen at least one significant interaction if sign epistasis or strong positive epistasis played a pervasive role in trait evolution. In contrast, we did find roles for gene-by-environment interactions involving pigmentation traits. Overall, our data suggest that the genetic architecture of adaptive traits often involves alleles of detectable effect, that strong epistasis does not always play a role in adaptation, and that environmental interactions can modulate the effect size of adaptive alleles.

## Introduction

Adaptive evolution is the result of natural selection, which acts by increasing the frequency of beneficial traits in a population. A number of important uncertainties persist regarding the genetic architectures of adaptive trait changes in nature, including the number and effect sizes of contributing variants, and their frequencies before and after the action of positive selection (Pritchard *et al.* 2010, Savoleinen *et al.* 2013, Barghi *et al.* 2020). Furthermore, research on the genetic basis of adaptation has largely been centered on the individual additive effects of each gene underlying the adaptive trait, whereas the role of gene-by-gene and gene-by-environment interactions in adaptation has remained more elusive (Whitlock *et al.* 1995, Malmberg & Mauricio 2005, Martin & Lenormand 2006, Bank 2022).

Theoretical and empirical studies have yielded varied findings concerning the number and strength of loci contributing to adaptive trait change. Fisher (1930) argued that traits were governed by numerous genetic variants of very small magnitude, and that natural selection proceeded via minute incremental changes in allele frequency at these loci. Extending Fisher's geometric model, Orr (1998) found that in a sequential model of genetic adaptation, a few larger effect sizes should tend to be followed by many smaller ones, yielding an exponential distribution of effects. However, adaptation in natural populations may sometimes depart from the assumptions of such models in multiple respects. First, the

role of standing variation (as opposed to new mutations) in the adaptive process continues to be investigated (Fuhrmann *et al.* 2023, Schlötterer 2023), and these two sources of genetic variation may differ in their effect sizes, dominance, and other properties (e.g. Orr & Betancourt 2001, Ségurel & Bon 2017, Bomblies & Peichel 2022). Second, the genetic architecture of local adaptation, in which populations in a heterogeneous landscape adapt to local conditions in the presence of migration, has a stronger bias towards alleles of large effect sizes (Griswold 2006, Yeaman & Whitlock 2011, Yeaman & Otto 2011). Third, interactions among genes impacting phenotypes (*i.e.* epistasis) may alter the dynamics of adaptive variants, as further discussed below.

In regards to the role of epistasis in adaptation, a discussion has existed since the onset of the Modern Synthesis, with some arguing that it is largely irrelevant to the trajectory of Darwinian selection (Fisher 1930, Cohan *et al.* 1989, Hill *et al.* 2008, Crow 2010) and others proposing that it plays an important role (Fenster *et al.* 1997, Hansen 2013, Wright 1931). The above literature suggests that on the one hand, epistasis might not be expected to strongly affect adaptation because alleles at unlinked loci can segregate independently and selection would act on the combined effect of each allele against different genetic backgrounds; and yet, epistasis has the potential to alter the rate at which adaptive trait changes can occur by producing larger or smaller effects in some of these backgrounds, and in

certain contexts, it may wield a stronger influence on the course of adaptation (Cohan *et al.* 1989, Crow 2010, Fenster *et al.* 1997, Fisher 1930, Hansen 2013, Hill *et al.* 2008, Wright 1931).

Epistasis has been shown to play a role in many evolutionary processes, including the evolution of sex and recombination, speciation, canalization, maintenance of genetic variation, and the evolution of co-adapted gene complexes (Hansen 2013). How epistatic interactions alter the response to directional selection is determined by the nature of the epistatic interaction (Hansen 2013). Some kinds of epistasis affect the magnitude of the phenotypic effects, such as positive and negative epistasis, and another kind, called sign epistasis, changes the direction of the effect. Multiple theoretical and simulation studies have investigated how each of these epistatic scenarios might influence the adaptive process (Carter *et al.* 2005; Hansen *et al.* 2006; Yukilevich *et al.* 2008; Barton 2017). For positive (synergistic) epistasis, in which the combined effect of both alleles is greater than the sum of the individual effects, additive genetic variance would increase, and the mean fitness in an adapting population is expected to change faster and reach a higher plateau than without epistasis. For negative epistasis, in which the combined effect is lower than the sum of the individual effects but still qualitatively consistent with the additive effects, additive genetic variance decreases and the mean fitness during adaptation changes more slowly and reaches a lower plateau than without

119 epistasis. Particularly in the context of adaptation, negative epistasis is also
120 referred to as diminishing returns epistasis. For sign epistasis, whether the
121 allele will contribute to a larger or smaller phenotype will depend on the
122 allele at another locus. In this case, the evolutionary dynamics can be more
123 complex, and the fate of one allele is attached to the other, but while both
124 variants persist, their interaction may impede adaptation. Furthermore, to
125 the extent that epistasis masks the phenotypic influence of some variants, it
126 may facilitate the accumulation of cryptic genetic variation for a given trait,
127 which may subsequently be exposed to selection when elements of the
128 genetic background (or the environment) change (Gibson & Dworkin 2004,
129 Steiner *et al.* 2007).

130 Despite the pervasiveness of epistasis at the genome-wide scale
131 (Huang *et al.* 2012), as well as between adaptive variants within proteins
132 (Lunzer *et al.* 2010, Gong & Bloom 2014, Starr & Thorthon 2016), the
133 prevalence of epistatic interactions among adaptive variants that contribute
134 to the evolution of more complex adaptive traits remains incompletely
135 understood. Studies of crop domestication have reported examples of
136 epistasis among artificially selected alleles, including grapevine varieties
137 (Duchêne *et al.* 2012) and many examples in maize domestication (Stitzer &
138 Ross-Ibarra 2018). Still, compared to wild alleles, domesticated alleles were
139 usually less sensitive to the genetic background (reviewed in Doust *et al.*
140 2014). Epistasis was also found among adaptive quantitative trait loci

141 (QTLs) underlying flowering time in *Arabidopsis thaliana* (Juenger *et al.*
142 2002). In a recent genome-wide screen in yeast, using genes known to be
143 involved in a high number of interactions, 24% of the adaptive variants were
144 strain-specific and indicative of epistasis (Ang *et al.* 2023). Positive epistasis
145 has been shown to underlie the evolution of bacteria with multiple
146 antibiotic resistance alleles (Trindade *et al.* 2009). Examples in animals
147 involve epistasis between alleles underlying adaptive coloration in
148 butterflies (Papa *et al.* 2013), negative epistasis for traits underlying fitness in
149 populations of *Drosophila melanogaster* experimentally selected on a
150 chronic larval malnutrition regimen (Vijendravarma & Kawecki 2013), and
151 epistasis between genes underlying coat color in oldfield mice, in which the
152 effect of one allele is only expressed in the presence of another allele
153 (Steiner *et al.* 2007).

154 The genetic architecture of adaptive traits can also be affected by
155 gene-by-environment interactions because the effect of a given allele can
156 change depending on its environment (Zeng *et al.* 1999, Mackay
157 2001). Transcriptome analysis of *D. melanogaster* reared at 20 different
158 environments have shown that expression of ~15% of genes changes
159 detectably with environment (Zhou et al. 2012). In some cases, gene-by-
160 environment interactions can be seen at the gene expression level but not
161 the metabolic level (Reed et al. 2014), highlighting the complexity of
162 interpreting its role in adaptation. Examples of interactions between the

environment and adaptive alleles include *D. melanogaster* reproductive performance at different temperatures (Fry *et al.* 1998), drought stress adaptation in wheat (Mathews *et al.* 2008), and local adaptation reflected in biomass for switchgrass (Lowry *et al.* 2019). Similarly to epistatic interaction, gene-by-environment interaction can also uncover cryptic genetic variation (Gibson & Dworkin 2004). The chaperone protein Hsp90 offers an example of how genetic and environmental interactions can uncover cryptic variation underlying discrete and continuous traits (Rutherford & Lindquist 1998, McGuigan & Sgro 2009, Flynn *et al.* 2020).

Here, we contribute to the understanding of the genetic architecture of adaptive traits and the emerging knowledge about genetic and environmental interactions by identifying adaptive quantitative trait loci (QTLs) underlying recent local adaptation in natural populations of *D. melanogaster* and asking whether there is evidence of epistasis among them and, for a subset, whether they interact with the environment. Using two newly-described panels of recombinant inbred lines (RILs), we investigate several traits that appear to have evolved directly or indirectly under adaptive differentiation between an ancestral range population (Zambia) and a population from either France or highland Ethiopia, regions colonized by *D. melanogaster* approximately 2 kya (Sprengelmeyer *et al.* 2020).

184 The traits examined here (cold tolerance, ethanol resistance,
185 pigmentation, song pattern, and wing length) show evidence of being either
186 direct targets of local adaptation or else pleiotropic readouts of local
187 adaptation targeting correlated traits. The pigmentation traits show strong
188 correlations with environmental variables, especially ultraviolet radiation
189 (Bastide *et al.* 2014), which reaches particularly high levels in the Ethiopian
190 highlands. Larger wings may help Ethiopian flies navigate in cooler,
191 thinner air, and wing size was found to show unusually strong quantitative
192 trait differentiation ($Q_{ST}$ = 0.985; Lande 1992; Spitze 1993) between the
193 Ethiopia and Zambia populations, compared to genome-wide genetic
194 differentiation (Lack *et al.* 2016), indicating a role for selection in this trait's
195 differentiation. France and Zambia have markedly different ethanol
196 resistance, also exceeding patterns of genome-wide genetic differentiation
197 (Sprengelmeyer *et al.* 2021). Cold developmental survival shows a similarly
198 consistent differentiation between France and Zambia in particular (Huang
199 *et al.* 2021), with clear presumptive adaptive value in light of climate
200 differences between these regions. A male song trait – the proportion of
201 pulses classified as slow (Clemens *et al.* 2018) – was included based on strong
202 population differentiation, with a $Q_{ST}$ of 0.797 exceeding the $F_{ST}$ of >96% of
203 non-singleton SNPs (Lollar *et al.* 2025). Although directional selection has
204 not been previously reported to have acted directly on song traits within *D.*
205 *melanogaster*, it is also possible that this trait difference reflects selection on

206 a pleiotropically connected trait, such as synaptic function in a novel
207 thermal environment (Pool *et al.* 2017).

208 We also note that for the pigmentation, size, and ethanol resistance
209 traits examined here, bulk mapping studies found that all of these
210 population trait changes had very different genetic architectures from one
211 mapping cross to the next (Bastide *et al.* 2016; Sprengelmeyer *et al.* 2021;
212 Sprengelmeyer *et al.* 2022). Given that the differences included QTLs with
213 effect size high enough to be detected across all the mapping crosses (Pool
214 2016), these results imply considerable segregating variation in genetic basis
215 of each trait difference within one or both of the populations studied.
216 However, it is possible (though as yet untested) that epistasis may also play a
217 role in yielding distinct QTLs in different mapping crosses for these traits.

218 For each of the above traits, we first identify QTLs and candidate
219 genes that may underlie each of these traits. Then, we quantify the strength
220 of evidence for epistasis impacting each detected QTL, and then assess the
221 overall signal of epistasis across traits. Lastly, we investigate the reaction
222 norm of the QTLs underlying a subset of the traits, related to pigmentation,
223 that were studied in two different temperature treatments. These
224 investigations provide new insights into both the genetic basis of adaptive
225 trait changes and the dependence of adaptive alleles on genetic interactions.

226

227 **Methods**

228 ***Mapping cross design***

229 We report two new Recombinant Inbred Line (RIL) mapping panels
230 of *Drosophila melanogaster*. Each RIL set was derived from a cross
231 between two inversion-free inbred lines from distinct geographic
232 populations, in each case pairing a strain from the southern-central African
233 ancestral range of the species (Sprengelmeyer *et al.* 2020) with a strain from
234 a cooler derived environment. One cross was between a Zambian inbred
235 line (ZI215N, BioProject PRJNA861300) and a highland Ethiopian inbred
236 line (EF43N, sequenced in Lack *et al.* 2016); the other was between a
237 different Zambian inbred line (ZI418N, sequenced in Sprengelmeyer & Pool
238 2021) and a French inbred line (FR320N, sequenced in Lack *et al.*
239 2016). Each cross was allowed to interbreed in an intercross design for 13
240 and 12 non-overlapping generations, in the Ethiopian and French cross,
241 respectively. Then, the offspring of individual females were inbred for 5
242 generations to create each RIL. We obtained 293 and 328 RILs for the
243 Ethiopian and French panels, respectively (BioProject PRJNA861300). The
244 Zambian lines were collected in Siavonga, the Ethiopian line was collected
245 in Fiche, and the French line was collected in Lyon (Lack *et al.* 2015). The
246 food used to rear the flies during the experiment and during the
247 phenotyping assays was prepared in batches of 4.5 L of water, 500 mL of
248 cornmeal, 500 mL of molasses, 200 mL of yeast, 54 g of agar, 45 mL of 10%
249 tegosept (in 95% ethanol), and 20 mL of propionic acid.

250
251 *Phenotypes*

252 Ethiopian flies have increased wing area, even after correcting size
253 relative to their larger body mass (Lack *et al.* 2016). We measured the wing
254 length of female flies that were at least 3-days old. 10 female flies per RIL
255 were photographed using an Amscope SM-4TZZ-144A dissection
256 microscope under $CO_2$ anesthesia. The pictures were scored with ImageJ
257 (Abramoff *et al.* 2004). Wing length was measured as the distance from the
258 intersection of the L4 longitudinal vein and the anterior cross vein to the L3
259 longitudinal vein intersection with the wing margin.

260 Ethiopian flies are darker than Zambian flies (Bastide *et al.* 2014). We
261 photographed and measured two to five females per RIL using a dissecting
262 scope. Resolution (3584 x 2748 pixels), gain (3.0), exposure time (99.84 ms),
263 magnification (20x), and illumination level were kept constant using an
264 Amscope adaptor for LED lamp at maximum lighting. White balance was
265 set at the same resolution using ColorChecker white balance. We measured
266 three common traits for pigmentation: the pigmentation of the
267 mesopleuron in greyscale proportion ranging from 0 for white to 1 for
268 black (herein, mesopleuron, a thorax trait), the pigmentation of the
269 background of the fourth abdominal segment in the same greyscale
270 proportion (herein, A4 Background), and the proportion of the fourth
271 abdominal segment that was covered by the black stripe (herein, stripe

272 ratio). Relatively low correlations (computed via regression) among these
273 three traits were observed among independent isofemale strains within the
274 Ethiopia and Zambia populations ($r < 0.35$), except for a higher correlation
275 between mesopleural and A4 Background for Ethiopia specifically ($r =$
276 0.646; Bastide *et al.* 2014).

277 Pigmentation is also plastically influenced by temperature, and the
278 Ethiopian population is located in a colder region, on a high plateau 3 km
279 above sea level. Therefore, we measured the three pigmentation traits in
280 flies raised at two temperatures (25 °C and 15 °C), to uncover potential
281 cryptic variation that could be present in the warmer Zambian (midpoint
282 temperature: 25 °C) but is only expressed in the colder Ethiopian (midpoint
283 temperature: 11 °C) population. We also report plasticity for these three
284 pigmentation traits, as the difference in the trait measured at 25 °C and
285 15 °C.

286 French flies have higher resistance to ethanol (Cohan & Graf 1985,
287 Sprengelmeyer & Pool 2021) and cold (Pool *et al.* 2017, Huang *et al.* 2021)
288 than Zambian flies. Ethanol resistance was measured as the average time
289 300 female flies, 3- to 5-day old, from each RIL needed to become
290 immobile when exposed to 18% ethanol. The flies were placed in 50 ml
291 falcon tubes with ethanol-saturated tissue placed on the bottom, and the
292 number of mobile flies was scored every 15 minutes for six hours. Cold
293 tolerance was measured as egg to pupa viability when raised at 15 °C. Given

294 that very few dead pupa were observed across RILs, this measure was taken
295 as a reasonable time-saving proxy for the egg to adult viability difference
296 previously demonstrated between the parental strains (Huang *et al.*
297 2021). To obtain this metric, six females and six males (3~5-day old) were
298 collected from each RIL and allowed to lay eggs for 15 hours. The egg to
299 pupa viability was estimated as the number of emerged adults plus left pupa
300 in a vial at Day 34~35 divided by the number of eggs present in the vial after
301 the parents were removed (Day 1).

302 The song pattern trait was the ratio of slow pulses over all pulses (slow
303 and fast) in the song made by males during courtship. Although not
304 expected to be under local environmental selection *a priori*, male courtship
305 is often under strong sexual selection. In addition, a large number of
306 nervous system genes appear to have evolved between warm- and cold-
307 adapted *D. melanogaster* populations (Pool *et al.* 2017), representing one
308 potential source of pleiotropic effects on song traits. We found that
309 Zambian male flies display a greater fraction of slow to fast pulses than
310 French flies (Lollar *et al.* 2025), a novel pulse mode classification recently
311 discovered within the *D. melanogaster* species complex (Clemens *et al.*
312 2018). The song data was recorded in the Stern Lab at Janelia Farms
313 Research Campus, using materials and methods described by Arthur and
314 colleagues (Arthur *et al.* 2013). Song was annotated without human
315 intervention with SongExplorer (Arthur *et al.* 2021). Annotations were

classified with locally modified versions of BatchSongAnalysis (https://github.com/dstern/BatchSongAnalysis), using previously trained *D. melanogaster* models provided by Ben Arthur (Lollar *et al.* 2025).

We expected that there might be some level of correlation among the traits of any given cross purely due to either linkage among causative variants or else pleiotropy. We calculated the pairwise correlation between all the traits measured for each cross to investigate the degree to which they are correlated.

### *DNA Extraction and Sequencing*

For each RIL, we extracted DNA from five to ten female flies from each line. The flies were crushed and homogenized using pipette tips in strip tubes, in a solution of 100 µl of lysis buffer (50 mM Tris-HCl with pH = 8, 100 mM EDTA, 100 mM NaCl, and 0.5% SDS) and 2 µl of proteinase K (IBI Scientific). The samples were incubated to inactivate the proteinase K (55 °C for 5 minutes, 95 °C for 10 minutes, and 25 °C hold). The supernatant of the fly lysate was transferred to new tubes, and we added SPRI beads (Sera-mag SpeedBeads SPRI beads, [GE Healthcare 24152105050250]) in a 1.8 to 1 proportion of beads to lysate. The beads were used in a solution of PEG 8000 (9 g), Tween 20 (27.5 µl), 5M NaCl, and 3 mL TE Buffer (composed of 100 µl of 1 mM EDTA, 500 µL of 10 mM Tris HCl). 1 mL of the beads were added to the buffer mix and filled with water until the final volume was

338 mL. The tubes were incubated for at least three minutes at room
339 temperature for DNA to bind to the beads and then placed on a magnetic
340 plate for five minutes to remove the beads from the solution. The
341 supernatant was discarded, and the beads were washed with two rounds of
342 80% ethanol (90 µL per well). DNA was eluted beads with 30 µL of $H_2O$ and
343 then used the magnetic plate to transfer only the resuspended DNA to new
344 tubes.

345 Genomic libraries were prepared following Adams *et al.* (2020), with
346 size selection, cutoff at 300 bp, and cleanup performed using the Zymo
347 Select-a-Size DNA clean & Concentrator [catalog No. D4080]. Libraries
348 were sequenced at the UW-Madison Biotechnology Center on the Illumina
349 NovaSeq 6000 platform, with 150 bp paired-end reads.

350

351 ***DNA Alignment and Ancestry Calling***

352 The reads were mapped to the *D. melanogaster* (v5.57) reference
353 genome using BWA-MEM, version 0.7.17 (Li 2013). We used Ancestry
354 HMM (Corbett-Detig & Nielsen 2017) to estimate ancestry along the
355 genome of each RIL, allowing for diploid ancestry calls (*i.e.* homozygous for
356 either parent, or heterozygous). Ancestries were summarized in non-
357 overlapping windows defined to contain 1,000 SNPs in the Zambian
358 population (19 kb average size), using the majority ancestry call in the case
359 of an ancestry breakpoint within the window. Window size was chosen to

360 ensure ample variation for ancestry calling within each window, and to
361 moderate the number of QTL and epistasis tests performed in order to
362 ensure computational tractability, while still allowing a genomic resolution
363 much narrower than the expected megabase scale ancestry tracts. When
364 two adjacent windows had the same ancestry genotype across all RILs, the
365 two windows were merged. We used a recombination map based on
366 Comeron *et al.* (2012) but modeled only one generation of recombination
367 when using Ancestry HMM, in order to focus on conservatively-defined
368 ancestry switches (pipeline available on
369 https://github.com/ribeirots/RILepi).
370
371 ***QTL Mapping***
372 To test whether adaptive loci showed evidence of epistatic
373 interactions we first used QTL mapping to identify the adaptive loci and
374 then performed epistasis tests between the focal loci and all other loci in the
375 genome. Each locus is a genomic window of ~19kb, defined and genotyped
376 as described above.
377 To identify loci underlying trait changes, we employed a similar
378 approach to the R/qtl (Broman *et al.* 2003) *scanone()* function, but with an
379 additive framework, modifying the genotypes to be coded as numeric
380 variables instead of categorical (https://github.com/ribeirots/RILepi), using
381 Python3 (Van Rossum & Drake 2009). The additive modification was

382 preferred in light of the small counts of specific genotypes due to the low
383 heterozygosity and the variable genomic ancestry skew present in our RIL
384 panels. We fit a model of the phenotype given the ancestry genotype of
385 each window (Trait ~ Marker). In our model, we coded the genotypes at Q
386 as numeric values: 0, 1, and 2 for the homozygous Zambian ancestry,
387 heterozygous ancestry, and Ethiopian or French homozygous ancestry,
388 respectively.

389 The initial QTL mapping is based on the comparison of a model with
390 a single QTL *versus* a model without any QTL, performed repeatedly one
391 locus at a time. For each locus, we obtained a logarithm of the odds (LOD)
392 score as the ratio between the log-likelihoods of the model with one QTL
393 over the model without a QTL. Because both RIL sets had average ancestral
394 frequencies skewed against the Zambian ancestry (68% Ethiopia ancestry
395 and 75% France ancestry), we excluded the windows with an ancestry bias of
396 90% or greater for either ancestry to avoid the effects of extremely uneven
397 sample sizes on the model. The genome-wide significance of a QTL was
398 tested using 10,000 permutations, in which trait values were randomly
399 shuffled. From each permutation, we saved the highest LOD score
400 obtained for any window (excluding windows with ancestry skew of 90% or
401 greater) and empirical LOD scores from each window were compared to
402 the null, permutation LOD score distribution. We considered the windows
403 whose LOD score's p-value was lower than 0.10 as putative QTLs (*i.e.* a less

404 than 10% chance of having a QTL signal of that strength anywhere in the
405 genome). A p-value threshold of 0.10 was chosen aiming to include a
406 sufficient number of QTLs to be tested for epistasis. We emphasize that
407 these QTL p-values are trait-specific, and do not attempt to quantify the
408 likelihood of any QTL peak for any analyzed trait having a given LOD
409 score.

410 Each putative QTL surrounded by windows with a lower LOD score
411 was considered a putative QTL peak. If two putative QTL peaks were not
412 separated by a window with a LOD score lower than the minor peak's LOD
413 score minus 1.5, the minor peak was removed. Finally, the remaining
414 putative QTL peaks were filtered to remove any peak within 10 cM of a
415 QTL peak with a higher LOD score, in order to increase the independence
416 of QTLs used in epistasis testing. The confidence interval for these QTLs
417 was defined as all contiguous windows with a LOD higher than the QTL's
418 peak LOD score minus 1.5. Heritability-based QTL effect ($h^2$) was
419 calculated as described in R/qtl for an intercrossing mapping design
420 (Broman *et al.* 2003).

421 The power of the QTL mapping analysis was calculated based on
422 simulated data for each RIL panel. We simulated a normally distributed
423 phenotype (mean = 0, standard deviation = 0.75) with additive effect of the
424 derived allele varying from 0.05 to 0.5 in 0.05 increments and without
425 dominance. We randomly sampled genotype distributions for each

426 simulation from the empirical RIL panels, to a total of 10,000 simulations
427 for each additive effect and RIL panel. We calculated the LOD score and
428 heritability-based QTL effect ($h^2$) for each simulation as described above,
429 and calculate its p-value based on the permutations of the empirical data for
430 each RIL panel. QTL mapping power was determined for each additive
431 effect and RIL panel as the proportion of simulations with p-value equal to
432 or lower than 0.1–the same threshold used in our analysis.
433
434 ***Candidate Genes and Population Genetics***
435 To identify genes potentially underlying the adaptive traits, we
436 scanned our QTL regions for signatures of local adaptation based on
437 population genetics. We sequenced genomes from inbred lines from each
438 of the studied populations to calculate a haplotype-based statistics: $\chi_{MD}$
439 (Lange & Pool 2016) and two $F_{ST}$ statistics (using Reynolds *et al.* 1983), $F_{ST_FullWin}$
440 (window-wide $F_{ST}$ calculated using all the SNPs in the window) and $F_{ST_MaxSNP}$
441 (the highest $F_{ST}$ value from a single SNP within the window), that have
442 power to distinct power to detect distinct kinds of selective events (da Silva
443 Ribeiro *et al.* 2022). We defined as outlier windows those that fell within the
444 top 1% of windows on the same chromosome arm for any of the above three
445 statistics. We focused on regions with recombination rates generally above
446 0.5 cM/Mb (Comeron *et al.* 2012) due to more localized signatures of
447 selection: 2.3–21.4 Mb of the chromosome X, 0.5–17.5 Mb of arm 2L, 5.2–

448 20.8 Mb of arm 2R, 0.6–17.7 Mb of arm 3L, and 6.9–26.6 Mb of arm 3R. We
449 selected as candidates all genes that overlapped with the outlier windows as
450 well as the first gene up- and down-stream of the outlier window, to
451 account for instances in which the target of selection is in a regulatory
452 region outside the gene region. We also identified other genes within these
453 QTLs with a known or potential association with the phenotype based on
454 FlyBase (release FB2023_05) annotation.
455
456 ***Epistasis Testing***
457 Epistasis tests were performed between each focal QTL and all of the
458 remaining genomic windows outside its confidence interval. The epistasis
459 test for each window pair consisted of an interaction LOD score obtained as
460 the ratio between the log-likelihoods of the model with two QTLs and their
461 interaction (Trait ~ Marker1 + Marker2 + Marker1:Marker2) *versus* a model
462 including both QTLs but no interaction (Trait ~ Marker1 + Marker2). The
463 interaction LOD score for each pair was compared against
464 permutations. Permutations were specific for each QTL analyzed. We
465 shuffled the phenotype, fixed the focal QTL (Marker1), and calculated the
466 interaction LOD score of Marker1 against all other windows in the
467 genome. The highest genome-wide interaction LOD score from each
468 permutation was kept and the empirical interaction LOD scores were
469 compared against this null, permuted interaction LOD distribution.

470
471 *Epistasis Meta-analysis*

472 We combined the results from all the epistasis tests across mapping
473 crosses and phenotypes to test the hypothesis of whether adaptive QTLs
474 have epistatic interactions. We collected the set of epistasis p-values from
475 each QTL and its most likely interactor, quantifying the probability of
476 obtaining any interaction term between that QTL and any partner locus in
477 the genome with an interaction LOD score as high as the one observed. We
478 used Fisher's combined probability test to ask if the p-values from each
479 QTL and their most likely interacting locus reject the null hypothesis that
480 there is no epistasis. The p-values should follow a uniform distribution if
481 the null hypothesis is true. Therefore, we performed an additional step to
482 investigate how many of the lowest p-values would need to be removed
483 from the data set to obtain a median value near 0.50, in order to ask
484 whether our cumulative data set showed any hints of epistasis across all
485 analyzed QTLs.

486
487 *Epistasis Power Analysis*

488 We calculated the power of our approach and our data sets to detect
489 an interaction by simulating phenotypes with different interaction
490 strengths. We chose one empirical QTL with intermediate sample size and
491 estimated the additive QTL effect among the detected QTL to serve as the
492 basis for the simulations. The QTL chosen was detected for the abdominal

493 background pigmentation at 25 °C, it had an estimated effect size equal to
494 0.035, mean trait value equal to 0.3485, and a standard deviation equal to
495 0.0697. The observed genotype distribution of the QTL peak window was
496 used for the simulations. Our null simulations generated phenotypes based
497 on a normal distribution with the observed trait mean and standard
498 deviation, and the simulated values were modified based on the trait effect
499 and individual genotypes (1x effect for heterozygous and 2x effect for non-
500 Zambian homozygous). We then calculated the interaction LOD score of
501 the focal peak window against all other genome windows outside the
502 original QTL's confidence interval and kept the highest genome-wide
503 interaction LOD score obtained. We repeated this process 10,000 times to
504 obtain a null (no interaction) distribution of interaction LOD scores.
505 To simulate epistasis, we used the genotype distribution of the
506 window most likely to be interacting with our focal QTL: the window with
507 the highest empirical interaction LOD score. We modified the empirical
508 effect of the focal QTL on the simulated phenotype based on the genotype
509 of the interacting genomic window. If the genotype of the interacting
510 window was Zambia homozygous, the original effect was not modified, if it
511 was non-Zambia homozygous, the original effect was multiplied by the
512 interacting factor $I$, and if it was heterozygous, the original effect was
513 intermediate (*i.e.* multiplied by $(1+I)/2$). The values of $I$ we simulated varied
514 from -2 to 4, depending on the nature of the epistatic interaction being

515 simulated. We simulated positive epistasis effects (original QTL effect
516 increased by the presence of the epistatic allele) with $I$ ranging from 1.125 to
517 4. For diminishing returns negative epistasis (original QTL effect decreased
518 by the presence of the epistatic allele), $I$ ranged from 0.889 (1/1.125) to
519 0.5. We simulated masking epistasis (the original QTL effect nullified in the
520 presence of the epistatic allele) with $I = 0$. Lastly, for sign epistasis (the
521 original effect changes in sign, *e.g.* instead of the non-Zambia QTL allele
522 producing larger trait it produces smaller traits), we examined effects from -
523 0.5 to -2.

524 Each interaction simulation was compared against the null
525 distribution and a p-value was calculated as the proportion of null
526 simulations with an interaction LOD score higher than the simulated
527 interacting LOD score. Power was calculated for each interaction effect $I$ as
528 the proportion of simulations that had p-value lower than 0.05.

529 We also calculated the power of our meta analysis based on 14 QTLs'
530 interaction p-values. For each interaction effect, we sampled 14 interaction
531 LOD score p-values and calculated (1) how often the fisher combined p-
532 value was as extreme or greater than the one we observed and (2) how often
533 at least one p-value was lower than the lowest p-value we obtained for our
534 empirical data.

535

536 ***Reaction Norms***

537 To investigate genotype-by-environment interactions for
538 pigmentation traits, we combined phenotypic data from RILs raised at the
539 two temperature treatments (15 °C and 25 °C) with the genotype of each
540 non-overlapping QTL. To test whether the genotype-by-environment
541 interaction was significant, we used a linear model with the phenotype as
542 the response variable and the genotype, environment, and genotype-by-
543 environment interaction as the explanatory variables.

544
545
546 **Results**

547 ***Genotype and phenotype data***

548 Whole genome sequences for the RILs had mean depth of coverage of
549 3.3X (S.D. 1.96 among RIL mean depths, Table S1) and 7.58X (S.D. 9.09,
550 Table S2) per site for EF and FR RILs, respectively, which should be more
551 than sufficient to call population ancestry in large chromosomal blocks
552 (Corbett-Detig & Nielsen 2017). Ancestries for both RIL sets were skewed
553 toward lower Zambian ancestry, with averages of 67.84% Ethiopian ancestry
554 and 77.88% French ancestry (full ancestry genotypes in Tables S3, S4 ). After
555 five generations of inbreeding, a low level of parental strain heterozygosity
556 was present in the final panel: 8.71% and 5.3% on the Ethiopian and French
557 panels, respectively (at the level of genomic windows). The sample size
558 varied for each trait based on the number of RILs successfully phenotyped
559 (Table 1, S1, S2).

560

561 **Table 1.** Summary of mapped traits. Listing the mapping cross used for each
562 trait (EF = Ethiopia, FR = France), the number of phenotyped lines for each
563 trait, the number of QTLs, and the number of QTLs with epistatic
564 interaction for each phenotypic trait.

| RIL panel | Trait | Sample size | # QTLs |
|---|---|---|---|
| EF | A4 Background 25 °C | 278 | 1 |
| EF | Stripe Ratio 25 °C | 278 | 1 |
| EF | Mesopleuron 25 °C | 278 | 1 |
| EF | A4 Background 15 °C | 190 | 0 |
| EF | Stripe Ratio 15 °C | 190 | 1 |
| EF | Mesopleuron 15 °C | 190 | 1 |
| EF | A4 Background (Plast.) | 178 | 0 |
| EF | Stripe Ratio (Plast.) | 178 | 0 |
| EF | Mesopleuron (Plast.) | 178 | 0 |
| EF | Wing Length | 268 | 5 |
| FR | Cold Tolerance | 304 | 0 |
| FR | Ethanol Resistance | 277 | 3 |
| FR | Song Pattern | 294 | 1 |

565

566 The distribution of the phenotypes were unimodal for all traits with
567 varying degrees of variance and low to moderate skew (Figures S1, S2).
568 Correlations among the analyzed traits were examined for each RIL panel,
569 which may indicate pleiotropy or else linkage of causative alleles. Among
570 pigmentation traits, the thoracic mesopleuron trait was strongly correlated
571 with abdominal background: r = 0.687 at 15 °C, r = 0.800 at 25 °C, r = 0.782

572 for the plasticity of these traits (Table S5). Stripe width showed moderate,
573 significant correlations with both of those traits at 25 °C ($r$ = 0.460, and $r$ =
574 0.253), but weaker correlations at 15 °C ($r$ = 0.169, and $r$ = -
575 0.085). Abdominal background showed a non-significant correlation
576 between the two temperatures, while the other two traits showed moderate,
577 significant correlations between temperatures. In light of the correlations
578 observed among many pigmentation traits, overlapping QTLs for
579 pigmentation traits were not treated as independent QTLs, and only the
580 QTL with the highest LOD score was used in downstream analyses. No
581 pigmentation trait was significantly correlated with wing length (Table S5),
582 the only other trait scored among the Ethiopian RIL panel. Among traits
583 scored from the French RIL panel, the song pattern was weakly correlated
584 with ethanol resistance, $r^2$ = 0.13 (Table S6).
585
586 ***Single locus QTL mapping***
587 We identified potential QTLs for eight out of the thirteen investigated
588 traits (Figure 1; Table 1). We list the genome-wide distribution of LOD
589 scores and p-values for each trait in the Table S7. We also present the
590 phenotypic distributions observed for each genotype at the QTL peak
591 window (Figures S3, S4) including the pulse song usage trait that is
592 discussed in more detail by Lollar *et al.* (2025). The traits with no detected
593 QTLs were A4 Background at 25 °C, all the three pigmentation plasticity

594 traits, and cold tolerance (genome-wide LOD scores shown in Figure S5).
595 The number of QTLs per trait ranged up to five, for wing length, with other
596 traits yielding one or three QTLs (Figure 1, Table 1). Twelve of the fourteen
597 QTLs were significant at $p < 0.05$, while two marginally significant QTLs -
598 one for A4 Background at 25 °C ($p = 0.0591$) and one QTL for ethanol
599 resistance ($p = 0.0693$) – were also considered in downstream analyses
600 (Table 2). The effect of each QTL, based on estimated $h^2$, varied from 0.033
601 to 0.285 and we had high power (>0.8) to detect QTLs of effect size 0.1
602 (Figure S6).

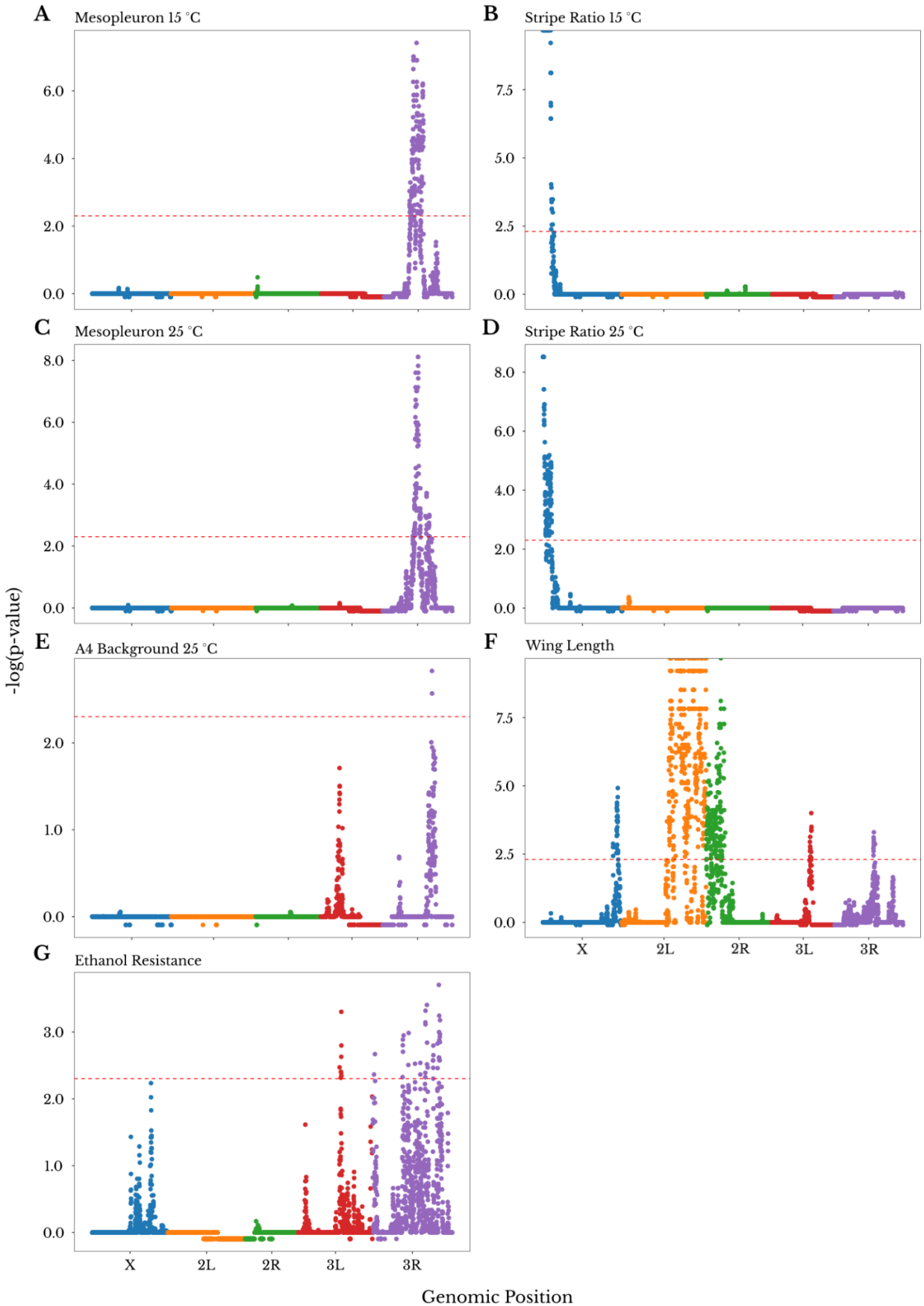
A
Mesopleuron 15 °C
B
Stripe Ratio 15 °C
C
Mesopleuron 25 °C
D
Stripe Ratio 25 °C
E
A4 Background 25 °C
F
Wing Length
G
Ethanol Resistance
-log(p-value)
X
2L
2R
3L
3R
Genomic Position

603

604 **Figure 1.** The number of QTLs for each trait ranged from 0 to 5. In this
605 figure, only the traits with at least one identified QTL are shown
606 (phenotype distributions for each genotype at each QTL peak window are
607 shown in Figures S3, S4); the traits without significant QTLs (Table 1) can be
608 seen in Figure S5. Each panel shows the -log of the (trait-specific) p-value
609 for the LOD score of the genomic windows. A4 Background (Figure 1E) is
610 shown here with no QTL above the threshold, but one marginally
611 significant QTL (p-value = 0.053, Table 2). Windows filtered out for
612 ancestry skew are given a value of -0.25. The red dashed line represents the
613 0.05 p-value cutoff based on 10,000 permutations. The color of the dots
614 represents the chromosome arm of each genomic window. Note that for
615 wing length, a single QTL spans a broad low recombination centromeric
616 region between 2L and 2R.
617
618 **Table 2.** Characteristics of detected QTLs for all analyzed phenotypes, and
619 possible underlying genes. The single QTL coefficient shows the
620 magnitude of phenotypic change by substituting one allele of the derived
621 population ancestry at that locus, which is shown on the scale of the
622 measured phenotype. The heritability due to the QTL ( $h^2$) shows how
623 much of the phenotypic variance is explained by the QTL (Broman *et al.*
624 2003). QTL p-value and epistasis p-value were obtained based on 10,000
625 permutations. * an estimated p-value of zero means the empirical value was

more extreme than any permutation. Q4 was excluded from subsequent meta-analysis due to a stronger overlapping QTL for a correlated trait. Further details of each QTL are given in Table S8. Candidate genes are given in light of a priori functional knowledge based on FlyBase annotation or as population genetic outliers for local adaptation statistics (n/a indicates that QTL was in a region of low recombination and was not analyzed for signatures of selection). Genes that may underlie the song trait are instead described by Lollar *et al.* (2025).

| RIL | Trait | QTL ID | LOD score | Trait Coeff | $h^2$ | QTL p-value | Epist. p-value | QTL Confidence Interval | Functional Candidate Genes | Genes with Signatures of Selection |
|---|---|---|---|---|---|---|---|---|---|---|
| EF | A4Back 25C | Q1 | 3.274 | 0.012 | 0.033 | 0.0591 | 0.736 | Chr3R:21614478 . 22512754 | | *TwdlQ, beat-vii, scrib* |
| EF | Mesopl 15C | Q2 | 5.819 | 0.012 | 0.112 | 0.0006 | 0.699 | Chr3R:16750589 . 16945416 | | |
| EF | Mesopl 25C | Q3 | 5.89 | 0.014 | 0.076 | 0.0003 | 0.714 | Chr3R:17549430 . 17666763 | *burs* | |
| EF | Stripe 25C | Q4 | 6.335 | 0.035 | 0.285 | 0.0002 | 0.643 | ChrX:1057169 . 2420139 | *Hr4, y* | n/a |
| EF | Stripe 15C | Q5 | 9.924 | 0.071 | 0.176 | 0* | 0.244 | ChrX:0 . 2141596 | *Hr4* | n/a |
| EF | Wing | Q6 | 9.581 | 0.026 | 0.109 | 0* | 0.322 | Chr2L:12902781 . 13046286 | | *Al6, Vha68-2, ACXE, CG16800, Tor, Ube4B* |
| EF | Wing | Q7 | 8.628 | 0.024 | 0.098 | 0* | 0.672 | Chr2L:22740849 . 23011543 | *Slmap* | n/a |
| EF | Wing | Q8 | 3.867 | 0.022 | 0.087 | 0.0183 | 0.444 | Chr3L:10353468 . 11407946 | *Cpr67Fa2, FoxK, Rbfox1, scyl, wls* | *Fad2, CG32079, klu* |

| | | | | | | | | | | |
|---|---|---|---|---|---|---|---|---|---|---|
| EF | Wing | Q9 | 3.526 | 0.019 | 0.059 | 0.0369 | 0.941 | Chr3R:18722896 . 19232530 | *Cow, Gbp3, hh, lrk1, p53, pnt, Rassf* | *Pnt* |
| EF | Wing | Q10 | 4.286 | 0.016 | 0.053 | 0.0073 | 0.183 | ChrX:20419847 . 20893609 | | *CG15450, Cyp6v1, hydra, shakB, CG1835, CG11227* |
| FR | EtOH | Q11 | 3.565 | 22.516 | 0.051 | 0.0368 | 0.208 | Chr3L:10829907 . 11166414 | *Aps* | *CG42831, tna* |
| FR | EtOH | Q12 | 3.253 | 27.506 | 0.127 | 0.0693 | 0.853 | Chr3R:3268049 . 3791969 | | n/a |
| FR | EtOH | Q13 | 3.74 | 19.166 | 0.038 | 0.0246 | 0.476 | Chr3R:23770233 . 24580087 | *fkh* | *trv, htt, CG34354, CG43125, snu* |
| FR | Song | Q14 | 9.111 | 0.019 | 0.079 | 0* | 0.273 | Chr3R:21997113 . 22171358 | | |

Of the five pigmentation QTLs, the two identified for stripe ratio (Q4 and Q5, at 25 °C and at 15 °C respectively) overlapped. We mapped the residuals values of the correlation between these two traits to investigate whether there was a signal beyond their correlation and did not obtain any significant QTLs (Figure S7). Therefore, only the overlapping QTL with the higher LOD score (15 °C) was retained for meta-analysis (Table S8). Confidence intervals for the two QTLs detected for mesopleuron (one at 25 °C and one at 15 °C) were separated by just over 600 kb, so they were kept as two independent QTLs for the meta-analysis (Table 2).

The direction of all QTLs (Table 2) was in the expected direction: substituting alleles of the derived population resulted in phenotypic

647 changes in the direction of the derived populations. This pattern is
648 congruent with a scenario where these QTLs are contributing to locally
649 adaptive trait changes (involving either the measured traits or else
650 pleiotropically correlated traits under selection), given that if the
651 phenotypic difference were neutral, we would expect some QTLs to show
652 an effect in the opposite direction (Orr 1998).
653

654 *Outlier and Candidate Genes within QTLs*

655 To generate hypotheses for possible causative genes underlying trait
656 changes, we used population genetic summary statistics to identify genes
657 within our QTLs that are potentially under local adaptation. Specifically,
658 we flagged genes associated with windows that fell within the chromosome
659 arm's top 1% of windows for window $F_{ST}$, maximum SNP $F_{ST}$, or the haplotype
660 statistic $\chi_{MD}$ (Table 2). These local adaptation scans were not conducted in low
661 recombination QTL regions due to the expected lack of gene-scale
662 resolution of selection signals in such genomic intervals. Since a striking
663 signal of local adaptation is not guaranteed at loci underlying these strong
664 population trait differences (*e.g.* if they involved soft partial sweeps), we also
665 noted the presence of other functionally relevant candidate genes within
666 each QTL.

667 We found a total of 26 candidate genes with functionally relevant
668 annotations on FlyBase related to their specific measured phenotype. Q3
669 (mesopleuron 25 °C) included the gene *burs* (Dewey *et al.* 2004), implicated
670 in cuticle tanning and hardening. Q4 and Q5 (the two stripe ratio
671 QTLs)both included the candidate gene *Hr4*, a gene that when suppressed
672 results in reduced pigmentation (Rogers *et al.* 2014). One also included the
673 gene *yellow*, canonically implicated in pigmentation variation and
674 evolution (e.g. Massey & Wittkopp 2015). This pair of QTLs overlapped
675 others previously detected for the same trait in distinct Ethiopia-Zambia

676 crosses (Bastide *et al.* 2016). The gene *ebony*, at which a soft sweep signal
677 associated with a pigmentation QTL was previously characterized for
678 Ethiopian *D. melanogaster* (Bastide *et al.* 2016), fell just between the closely-
679 located Q2 and Q3 (mesopleuron 15 °C and 25 °C).

680 At least one gene related to wing development was found within each
681 of the five wing length QTL regions. Within Q6 (on arm 2L), our
682 population genetic outliers included the *mechanistic Target of rapamycin*
683 gene (*mTor*), which plays a key role in insulin signaling and growth
684 regulation, and has been tied to wing size and development specifically
685 (Parker & Struhl 2015). Outliers inside this QTL also included the potential
686 wing regulators *Vha68-2* and *Ube4B* (Krupp *et al.* 2005, Blanco *et al.* 2010,
687 Okada *et al.* 2016, López-Varea *et al.* 2021). Within Q7 (low recombination
688 regions of 2L), among the few genes present was *Slmap*, a hippo signaling
689 gene shown to alter wing size (Zheng *et al.* 2017). Within Q8 (3L),
690 population genetic outliers included *klu*, which regulates cell size and
691 proliferation, and is associated with wing size defects (Schertel *et al.*
692 2015). Within Q9 (3R), outliers included *pnt*, related to wing morphogenesis
693 (Dworkin & Gibson, 2006, Bejarano *et al.* 2008, Paul *et al.* 2013). The X-
694 linked wing QTL (Q10) included an outlier gene possibly involved in wing
695 development, *shakB* (Krishnan *et al.* 1993). Q7, Q8, and Q10 overlap with
696 previously detected wing length QTLs, each from a different Ethiopia-

697 Zambia cross out of four previously analyzed mapping crosses
698 (Sprengelmeyer *et al.* 2022).
699 For the ethanol resistance QTLs, we identified two population genetic
700 outlier genes (*htt* and *trv*) previously implicated in response to ethanol
701 (Fochler *et al.* 2017) within Q13 (3R). Outlier genes detected within the other
702 two QTLs had no annotated connection to ethanol. These QTLs did not
703 overlap with those previously detected for the same trait from distinct
704 France-Zambia crosses (Sprengelmeyer *et al.* 2021), in line with the
705 genetically variable basis of this trait identified by that study.
706 Overall, we identified both novel candidate genes associated with the
707 detected QTLs and genes that had already been implicated with their
708 respective trait. The identification of genes already known to underlie these
709 traits (although in many cases not their evolution) provides support for the
710 approach we used here.
711
712 ***Epistasis***
713 To investigate whether there is evidence of epistasis among adaptive
714 loci, we performed an epistasis scan for each single QTL and a meta-
715 analysis combining the results across non-correlated traits. We did not
716 identify any individually significant epistatic QTL pairs. The lowest
717 genome-wide interaction LOD score p-value we obtained was 0.183, for a
718 wing length QTL (Table 2).

719 Our meta-analysis of the combined non-overlapping single QTLs also
720 supports the hypothesis that there is no strong epistasis involving adaptive
721 loci. By combining the interaction p-values for all non-overlapping QTLs
722 (where each p-value denotes the probability of that QTL having any
723 interaction LOD effect that strong in the genome, based on 10,000
724 permutations), we obtained a p-value of 0.763 using Fisher's combined
725 probability test. This result indicated that the observed p-values do not
726 deviate from the null expectation of uniformly distributed p-values
727 expected without epistasis involving adaptive loci.

728 Because our sample sizes of RILs may not be suitable for detecting all
729 magnitudes of epistasis, we conducted a simulation-driven analysis to
730 indicate the strength of our negative results, and to indicate if there was a
731 parameter space of epistasis that we could confidently rule out based on
732 these results. Based on this analysis, our method had a high power (over
733 80%) to detect an epistatic QTL pair in scenarios of sign epistasis, in which
734 the interaction effect changed the direction of the main effect, as well as
735 high power to detect strong positive epistasis in which the interaction
736 effected increased the main effect at least 2.5-fold (Figure 2, Table S9). We
737 also tested the power of our meta-analysis by re-sampling 13 p-values from
738 simulated data sets of different interaction effects (Figure 2). This analysis
739 indicated that we should have had power to detect similar scenarios of
740 strong epistasis as indicated for the lowest p-value analysis above (*i.e.* sign

epistasis and positive epistasis at least doubling the main effect, and that we would likely have detected masking epistasis as well, in which the main effect was erased by the modifier). Therefore, although the power to detect moderate and weak epistasis is reduced rapidly, the lack of detected epistatic interactions from our empirical data supports the hypothesis that strong forms of epistasis did not play an important role in these instances of evolution.

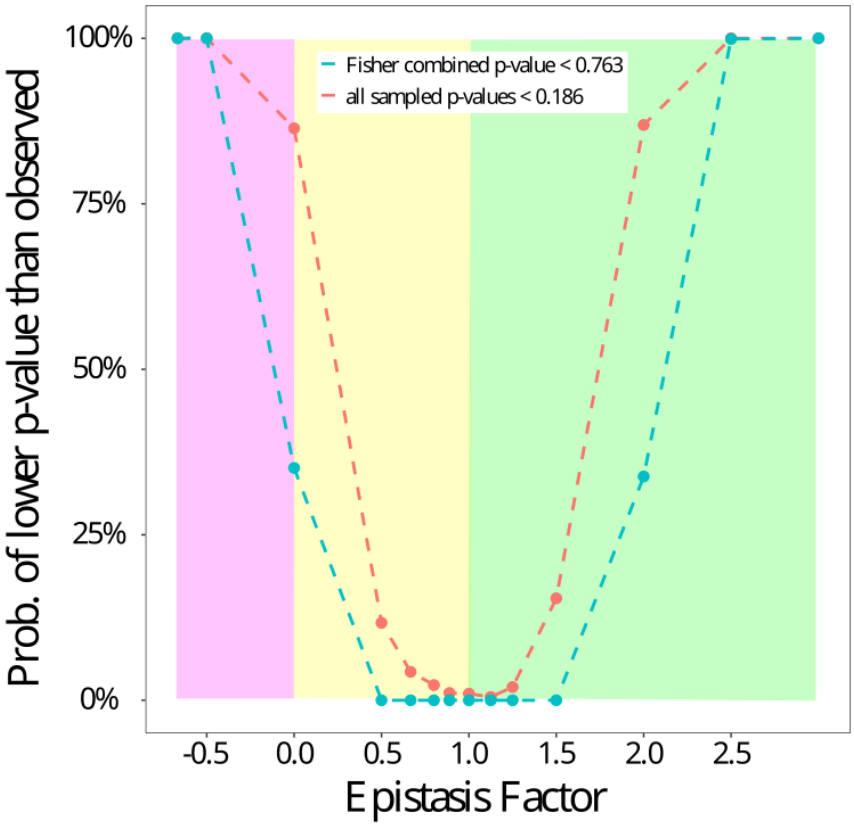


**Figure 2.** Simulation analysis indicating that strong positive epistasis or sign epistasis should have been detectable for the empirical data. Simulations based on randomly permuted individual genotypes and simulated epistatic effects (see Materials and Methods) were conducted to assess our ability to

753 detect varying models of epistasis based on either the lowest empirical
754 epistasis p-value (red series) or the Fisher-combined epistasis p-value across
755 13 analyzed QTLs (blue series). Here, the epistasis factor (x-axis) represents
756 the multiplier that a modifier locus exerts on the primary QTL's
757 effect. Thus, negative values represent sign epistasis (pink shaded area),
758 zero represents masking epistasis, values between 0 and 1 indicate negative
759 epistasis (yellow shaded area), and values above 1 indicate positive epistasis
760 (green shaded area). The y-axis shows the proportion of occurrences out of
761 the 1,000 resampled instances in which a given model of epistasis yielded a
762 lowest p-value lower than the observed 0.183 (red), or else how often the
763 combined Fisher p-value was lower than the observed 0.763 (blue).
764

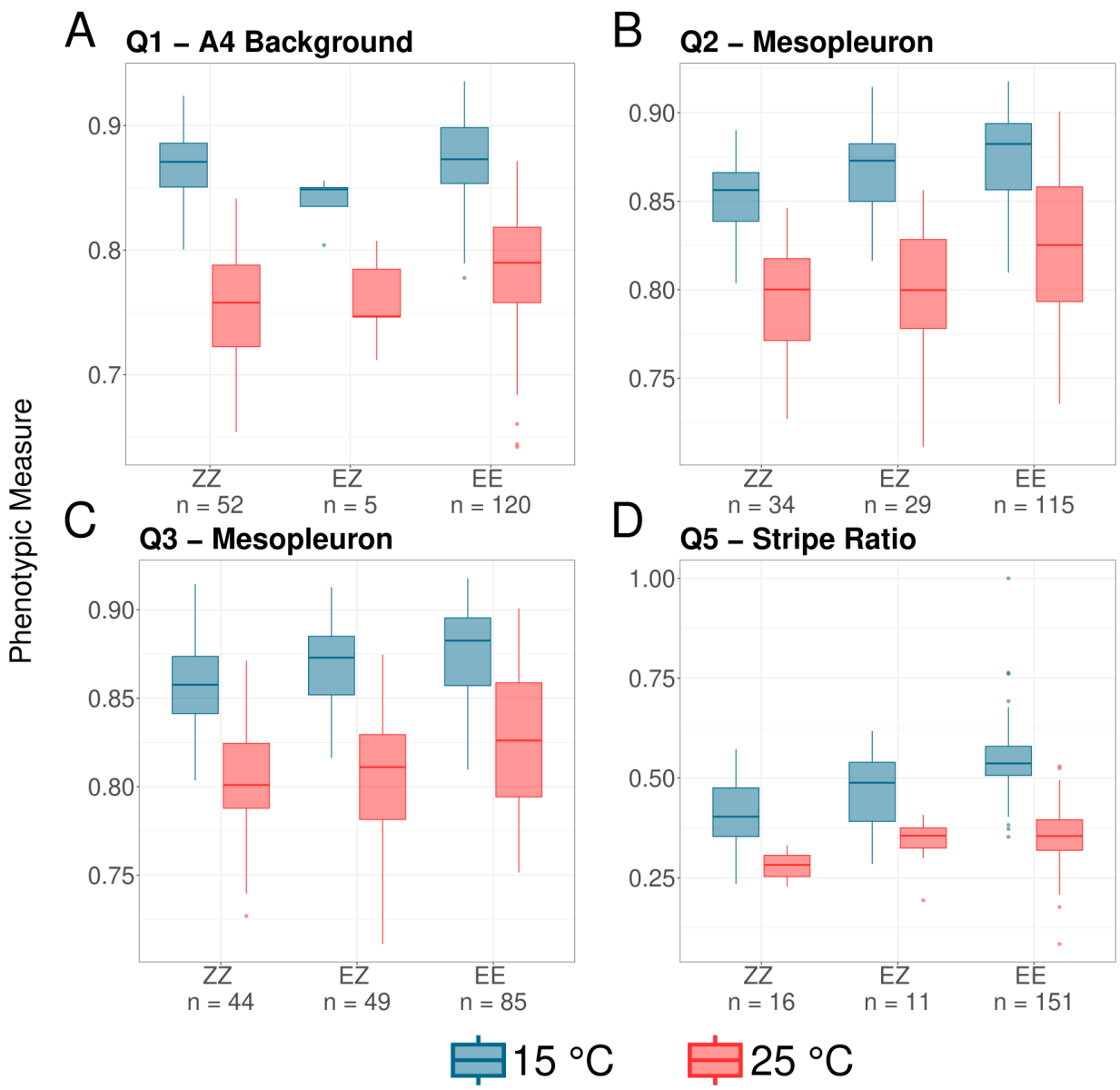


**Figure 3.** The reaction norms of the four non-overlapping pigmentation QTL show darker phenotypes for flies raised at 15 °C than at 25 °C and for flies with Ethiopia ancestry alleles, corroborating expectations. (A) Q1: A4 Background at 25 °C, with peak centered near 21.6 Mb on 3R. (B) Q2: Mesopleuron at 15 °C, near 16.8 Mb on 3R. (C) Q3: Mesopleuron at 25 °C, near 17.6 Mb on 3R. (D) Q5: Stripe ratio at 15 °C, near 1.3 Mb on the X. The

772 y-axis shows the mean phenotype for each genotype and temperature
773 treatment; a higher number is a darker phenotype. ZZ = Zambia
774 homozygous, EZ = heterozygous, EE = Ethiopia homozygous.
775

776 ***Phenotype plasticity for pigmentation QTLs***

777 Fly pigmentation is known for its temperature-based plasticity; flies
778 reared at lower temperatures develop darker phenotypes than those raised
779 at warm temperatures (David *et al.* 1990). Our results recapitulated this
780 behavior, in that average pigmentation traits were higher (*i.e.* darker) at
781 15 °C (Figure 3). We identified one overlapping QTL for stripe ratio at both
782 temperatures (Table 2). Based on the trait correlation and the shared QTL,
783 at least part of the genetic architecture underlying adaptive melanism
784 appears to be shared between temperatures.

785 The reaction norm of four pigmentation QTLs also showed that flies
786 raised at 15 °C showed darker phenotypes for all traits and even darker
787 phenotypes for the Ethiopia homozygotes, as expected (Figure 3). We also
788 found significant genotype-by-environment interactions for two of these
789 QTLs – A4 Background ($p = 0.003$) and stripe ratio ($p = 0.007$) (Figure
790 3A,D). The change in stripe ratio (Figure 3D) was greater for flies with the
791 homozygous Ethiopia genotype. Here, the more derived-like environment
792 appears to enhance the phenotypic consequences of the Ethiopian
793 pigmentation variants. In contrast, for the A4 Background QTL, the

794 phenotype means at 15 °C only show a small difference between
795 homozygous genotypes, compared to a larger difference at 25 °C, which is
796 congruent with this QTL being found only at 25 °C (whereas differences in
797 the heterozygote means may reflect small sample size effects).

798
799

800 **Discussion**

801 We report the creation of two new *Drosophila melanogaster* RIL
802 panels established from crosses between single inbred lines from Ethiopia
803 and Zambia, and from France and Zambia. We used these new data sets,
804 together with an updated QTL mapping approach focusing on additive
805 effects, to investigate the genetic architectures of multiple traits that have
806 evolved to become differentiated between *D. melanogaster*
807 populations. We did not find evidence for strong epistasis underlying their
808 evolution, but genotype-by-environment interactions were supported for
809 two of the three traits investigated.

810
811 ***Genetic architectures underlying trait evolution***

812 Our QTL mapping results indicate genetic architectures for most
813 traits involving detectable loci with non-trivial effect sizes (5.3% to 21.4%;
814 Table 2), consistent with past bulk mapping studies for some of these traits
815 (Bastide *et al.* 2016, Sprengelmeyer *et al.* 2020, Sprengelmeyer *et al.*
816 2021). In combination with those studies, our results reinforce previous

817 findings that evolved populations maintain persistent variability in the
818 genetic basis of pigmentation traits, wing length, and ethanol resistance. We
819 did not find significant QTLs for cold tolerance or thermal plasticity of
820 pigmentation, which could reflect either a more complex genetic basis of
821 those traits or else greater non-genetic variance in those assays.

822 We have also identified genes within the detected QTLs that might be
823 underlying the relevant traits, including genes previously known to be
824 related to the phenotype and, with the use of population genetic signatures
825 of selection, novel candidate genes (Table 2). The identified genes
826 represent viable hypotheses for contributors to the genetic architecture of
827 traits that appear to have evolved due to local adaptation targeting either
828 these or pleiotropically correlated traits but deserve further
829 investigation. Additional studies using functional approaches such as
830 genome editing will be needed to confirm the roles of these genes in the
831 evolution of the respective traits.

832
833 ***Lack of evidence for epistasis***

834 Despite the pervasiveness of epistasis underlying the genetic basis of
835 complex traits (Huang *et al.* 2012, Mackay 2014), we did not find evidence of
836 epistasis involving any of the detected adaptive loci (Table 2). In light of
837 our power analysis (Figure 2), our empirical results primarily argue against
838 the presence of modifier variants within our RIL panels that trigger sign

839 epistasis, complete masking epistasis, or strong positive epistasis with regard
840 to the main effect loci. In contrast, our study does not speak to the presence
841 of quantitatively negative epistasis (*e.g.* diminishing returns epistasis) or
842 more moderate positive synergistic epistasis.

843 Previous studies have also found mixed results when investigating
844 epistatic interaction among adaptive loci (Malmberg & Mauricio 2005). In
845 some cases, the varied outcome for adaptive traits might reflect the
846 transient nature of epistatic interactions in a population, given that the
847 epistatic effects of two loci on a trait depend on the allele frequency of the
848 interacting alleles. Interestingly, studies mapping QTLs for fitness-related
849 traits (more directly related to reproduction and survival) have a more
850 consistent result, often showing more epistatic QTLs than additive QTLs
851 (Malmberg & Mauricio 2005).

852 One of the difficulties in extrapolating the results of experimental
853 crosses to natural populations is that experimental crosses start with a
854 limited amount of genetic variation (Mackay 2014). In our case, the crosses
855 were made between one inbred line from each parental population, which
856 will exclude some variants present in the source populations while elevating
857 some naturally rare variants to moderate frequency. Previous genetic
858 mapping studies of traits such as pigmentation (Bastide *et al.* 2016), ethanol
859 resistance (Sprengelmeyer *et al.* 2021), and wing size (Sprengelmeyer *et al.*
860 2022) have shown that single crosses made with different inbred lines from

861 the same population do not contain most of the genetic variation
862 underlying population differentiation in each trait. However, our crosses
863 have the advantage of focusing on a simplified genetic architecture, which
864 may improve power to detect interactions among the variants present, in
865 addition to clear inference of the parental origin of alleles genomewide.
866 We highlight that our study likely underestimates the epistatic
867 interactions affecting *D. melanogaster* adaptive traits, since we only had
868 power to detect relative strong interactions (Figure 2, Table S9). Based on
869 the limited numbers of RILs available, we could only detect strong additive
870 QTLs, and we needed to focus our epistasis scan on interactions with those
871 few strong QTLs. Future research with a larger sample size (e.g. Torgeman
872 & Zamir 2023) would be helpful to achieve more extensive insights into the
873 scope of epistatic interactions affecting traits such as these. Studies using a
874 more diverse set of starting lineages could mitigate some of the issues
875 related to the limited genetic variation in our study. Additionally, drawing
876 information from diverse sources, such as genome-wide association studies,
877 bulk segregating approaches, and population genetics signatures of selection
878 could be useful in designing mapping studies capable of not only
879 identifying QTLs but candidate loci within QTLs. Multi-trait QTL mapping
880 could also be a fruitful future direction to investigate the role of epistasis on
881 adaptations as it can increase mapping power (Pitchers *et al.* 2019). Multi-
882 trait approaches can also infer pleiotropy and epistasis (Zhang *et al.* 2016),

883 adding a layer of complexity to the interpretation of results that could be
884 especially challenging when some of the measured traits are not expected to
885 have similar developmental and genetic bases.
886
887 ***Genetic Architectures at Two Temperatures***
888 Although the three body pigmentation traits we studied were
889 somewhat correlated (Table S5), no shared QTL was noted between them
890 (Table 2). Instead, we found two instances of overlapping or neighboring
891 QTLs for the same trait measured at different temperatures, with 25 °C and
892 15 °C being more similar to the mean temperatures in the Zambian and
893 Ethiopian populations, respectively. These results are compatible with the
894 same or nearby genes being responsible for pigmentation differences at
895 both temperatures.
896 *Drosophila* pigmentation is known to show thermal plasticity, and
897 Ethiopian flies would have been expected to become somewhat darken on
898 this basis alone, and yet they have also adapted genetically to become
899 darker (Bastide *et al.* 2014). It is unclear whether this pigmentation plasticity
900 is adaptive, which in itself can facilitate adaptive evolution (Ghalambor *et al.*
901 2007). Unlike larger ectotherms, it has been estimated that the solar gain in
902 temperature from having dark pigmentation is at most a fraction of a
903 degree for an organism with the small size and high surface to volume ratio
904 of *Drosophila* (Willmer & Unwin 1981, Hirai & Kimura 1997). Across African

905 populations of *D. melanogaster*, levels of ultraviolet radiation have been
906 found to be stronger predictors of pigmentation than temperature (Bastide
907 *et al.* 2014).

908 Gene-by-environment loci have recently been shown to be enriched
909 for signatures of positive selection (Lea *et al.* 2022), supporting the
910 hypothesis that environment-specific loci play an important role in local
911 adaptation. Here, we did find that two QTLs underlying pigmentation
912 evolution showed significant genotype-by-environment interactions
913 (Figure 3), suggesting that the rate of their response to selective events
914 might have changed upon colonization of colder environments. However,
915 we did not find consistent patterns of either gene-by-gene or gene-by-
916 environment interactions that met the predictions of cryptic variation. For
917 example, the absence of epistatic interactions means that the Ethiopian
918 alleles did not have their effect completely masked or reversed by another
919 gene on the ancestral background. And in the case of gene-environment
920 interactions, there was an enhanced QTL effect in the derived Ethiopia-like
921 cool environment in just one of two significant cases (*i.e.* the stripe
922 QTL). While cryptic variation may have played a role in the evolution of
923 some or all of these traits, our results suggest that it may not have been
924 pervasive with respect to the strongest effect changes.

925

926 **Conclusion**

While the genetic architecture underlying adaptive evolution may vary somewhat depending upon the trait, there remains a key interest in assessing potentially general patterns. In combination with past studies, our results suggest that most adaptive trait changes involve variants of non-trivial effect size, and that these variants often do not initially reach fixation. Epistasis is an important component underlying complex traits, including in flies (Huang *et al.* 2012), but we did not find evidence that strong epistasis was relevant for the adaptive evolution of the studied loci. In light of the existence of other examples in which epistasis among adaptive loci have been shown (Malmberg & Mauricio 2005), our study highlights that the answer to the classic debate on whether epistasis is important to natural selection might vary case by case. Lastly, we found evidence of gene-by-environment interactions underlying pigmentation, stressing that the variability of genetic architectures can also be environment-dependent, which is particularly relevant in light of rapidly changing global environments.

**Data availability**: Source code used in the analyses is available on GitHub (https://github.com/ribeirots/RILepi). Raw sequence read data for the Recombinant Inbred Lines are available on the Sequence Read Archive (BioProject: PRJNA861300).

**Acknowledgments**: We thank members of the Pool lab for helpful comments on this manuscript.

**Conflict of interest**: The authors declare no conflict of interest.

**Funding:** This research was funded by NIH grants R01 GM127480 and R35 GM136306.

## References


Abramoff, M. D., Magalhães, P. J., & Ram, S. J. (2004). Image processing with ImageJ. Biophotonics International, 11(7), 36–42.

Adams, M., McBroome, J., Maurer, N., Pepper-Tunick, E., Saremi, N. F., Green, R. E., Vollmers, C., & Corbett-Detig, R. B. (2020). One fly–one genome: chromosome-scale genome assembly of a single outbred *Drosophila melanogaster*. Nucleic Acids Research, 48(13), e75-e75. doi:10.1093/nar/gkaa450.

Ang, R. M. L., Chen, S. A. A., Kern, A. F., Xie, Y., & Fraser, H. B. (2023). Widespread epistasis among beneficial genetic variants revealed by high-throughput genome editing. Cell Genomics, 3(4). doi:10.1016/j.xgen.2023.100260.

Arthur, B. J., Ding, Y., Sosale, M., Khalif, F., Kim, E., Waddell, P., Turaga, S. C., & Stern, D. L. (2021). SongExplorer: A deep learning workflow for discovery and segmentation of animal acoustic communication signals (p. 2021.03.26.437280). bioRxiv. doi:10.1101/2021.03.26.437280.

Arthur, B. J., Sunayama-Morita, T., Coen, P., Murthy, M., & Stern, D. L. (2013). Multi-channel acoustic recording and automated analysis of *Drosophila* courtship songs. BMC Biology, 11(1), 11. doi:10.1186/1741-7007-11-11.

Bank, C. (2022). Epistasis and adaptation on fitness landscapes. Annual Review of Ecology, Evolution, and Systematics, 53, 457-479. doi:10.1146/annurev-ecolsys-102320-112153.

Barghi, N., Hermisson, J., & Schlötterer, C. (2020). Polygenic adaptation: a unifying framework to understand positive selection. Nature Reviews Genetics 21(12), 769-781. doi:10.1038/s41576-020-0250-z.

Barton, N. H. (2017). How does epistasis influence the response to selection? Heredity, 118(1), 96-109. doi:10.1038/hdy.2016.109.

Bastide, H., Lange, J. D., Lack, J. B., Yassin, A., & Pool, J. E. (2016). A variable genetic architecture of melanic evolution in *Drosophila melanogaster*. Genetics, 204(3), 1307–1319. doi:10.1534/genetics.116.192492.

Bastide, H., Yassin, A., Johanning, E. J., & Pool, J. E. (2014). Pigmentation in *Drosophila melanogaster* reaches its maximum in Ethiopia and correlates most strongly with ultra-violet radiation in sub-Saharan

Africa. BMC Evolutionary Biology, 14(1), 179. doi:10.1186/s12862-014-0179-y.

Bejarano, F., Luque, C. M., Herranz, H., Sorrosal, G., Rafel, N., Pham, T. T., & Milán, M. (2008). A gain-of-function suppressor screen for genes involved in dorsal–ventral boundary formation in the *Drosophila* wing. Genetics, 178(1), 307-323.. http://dx.doi.org/10.1534/genetics.107.081869.

Blanco, E., Ruiz-Romero, M., Beltran, S., Bosch, M., Punset, A., Serras, F., & Corominas, M. (2010). Gene expression following induction of regeneration in *Drosophila* wing imaginal discs. Expression profile of regenerating wing discs. BMC Developmental Biology, 10(1), 1-14. http://dx.doi.org/10.1186/1471-213X-10-94.

Bomblies, K., & Peichel, C. L. (2022). Genetics of adaptation. Proceedings of the National Academy of Sciences, 119(30), e2122152119. doi:10.1073/pnas.2122152119.

Broman, K. W., Wu, H., Sen, Ś., & Churchill, G. A. (2003). R/qtl: QTL mapping in experimental crosses. Bioinformatics, 19(7), 889–890. doi:10.1093/bioinformatics/btg112.

Carter, A. J., Hermisson, J., & Hansen, T. F. (2005). The role of epistatic gene interactions in the response to selection and the evolution of evolvability. Theoretical Population Biology, 68(3), 179-196. doi:10.1016/j.tpb.2005.05.002.

Clemens, J., Coen, P., Roemschied, F. A., Pereira, T. D., Mazumder, D., Aldarondo, D. E., Pacheco, D. A., & Murthy, M. (2018). Discovery of a new song mode in *Drosophila* reveals hidden structure in the sensory and neural drivers of behavior. Current Biology, 28(15), 2400-2412.e6. doi:10.1016/j.cub.2018.06.011.

Cohan, F. M., & Graf, J.-D. (1985). Latitudinal cline in *Drosophila melanogaster* for knockdown resistance to ethanol fumes and for rates of response to selection for further resistance. Evolution, 39(2), 278–293. doi:10.2307/2408362.

Cohan, F. M., Hoffmann, A. A., & Gayley, T. W. (1989). A test of the role of epistasis in divergence under uniform selection. Evolution, 43(4), 766-774. doi:10.2307/2409305.

1023 Comeron, J. M., Ratnappan, R., & Bailin, S. (2012). The many landscapes of
1024 recombination in *Drosophila melanogaster*. PLOS Genetics, 8(10),
1025 e1002905. doi:10.1371/journal.pgen.1002905.

1026 Corbett-Detig, R., & Nielsen, R. (2017). A hidden Markov model approach
1027 for simultaneously estimating local ancestry and admixture time using
1028 next generation sequence data in samples of arbitrary ploidy. PLoS
1029 Genetics, 13(1), e1006529. doi:10.1371/journal.pgen.1006529.

1030 Crow, J. F. (2010). On epistasis: why it is unimportant in polygenic
1031 directional selection. Philosophical Transactions of the Royal Society B:
1032 Biological Sciences, 365(1544), 1241–1244. doi:10.1098/rstb.2009.0275.

1033 da Silva Ribeiro, T., Galván, J. A., & Pool, J. E. (2022). Maximum SNP $F_{ST}$
1034 outperforms full-window statistics for detecting soft sweeps in local
1035 adaptation. Genome Biology and Evolution, 14(10), evac143.
1036 doi:10.1093/gbe/evac143.

1037 David, J. R., Capy, P., & Gauthier, J.-P. (1990). Abdominal pigmentation and
1038 growth temperature in *Drosophila melanogaster*: similarities and
1039 differences in the norms of reaction of successive segments. Journal of
1040 Evolutionary Biology, 3(5–6), 429–445. doi:10.1046/j.1420-
1041 9101.1990.3050429.x.

1042 Dewey, E. M., McNabb, S. L., Ewer, J., Kuo, G. R., Takanishi, C. L., Truman,
1043 J. W., & Honegger, H. W. (2004). Identification of the gene encoding
1044 bursicon, an insect neuropeptide responsible for cuticle sclerotization
1045 and wing spreading. Current Biology, 14(13), 1208-1213..
1046 http://dx.doi.org/10.1016/j.cub.2004.06.051.

1047 Doust, A. N., Lukens, L., Olsen, K. M., Mauro-Herrera, M., Meyer, A., &
1048 Rogers, K. (2014). Beyond the single gene: How epistasis and gene-by-
1049 environment effects influence crop domestication. Proceedings of the
1050 National Academy of Sciences, 111(17), 6178-6183.
1051 doi:10.1073/pnas.1308940110.

1052 Duchêne, E., Butterlin, G., Dumas, V., & Merdinoglu, D. (2012). Towards the
1053 adaptation of grapevine varieties to climate change: QTLs and candidate
1054 genes for developmental stages. Theoretical and Applied Genetics, 124(4),
1055 623-635. doi:10.1007/s00122-011-1734-1.

1056 Dworkin, I., & Gibson, G. (2006). Epidermal growth factor receptor and transforming
1057 growth factor-β signaling contributes to variation for wing shape in *Drosophila*

*melanogaster*. Genetics, 173(3), 1417-1431. http://dx.doi.org/10.1534/genetics.105.053868.

Fenster, C. B., Galloway, L. F., & Chao, L. (1997). Epistasis and its consequences for the evolution of natural populations. Trends in Ecology & Evolution, 12(7), 282–286. doi:10.1016/S0169-5347(97)81027-0.

Fisher, R. A. (1930). The genetical theory of natural selection (pp. xiv, 272). Clarendon Press. doi:10.5962/bhl.title.27468.

Flynn, J. M., Rossouw, A., Cote-Hammarlof, P., Fragata, I., Mavor, D., Hollins III, C., Bank, C., & Bolon, D. N. (2020). Comprehensive fitness maps of Hsp90 show widespread environmental dependence. Elife, 9, e53810. doi:10.7554/eLife.53810.

Fochler, S., Morozova, T. V., Davis, M. R., Gearhart, A. W., Huang, W., Mackay, T. F., & Anholt, R. R. (2017). Genetics of alcohol consumption in *Drosophila melanogaster*. Genes, Brain and Behavior, 16(7), 675-685. doi:10.1111/gbb.12399.

Fry, J. D., Nuzhdin, S. V., Pasyukova, E. G., & Mackay, T. F. (1998). QTL mapping of genotype–environment interaction for fitness in *Drosophila melanogaster*. Genetics Research, 71(2), 133-141. doi:10.1017/S0016672398003176.

Fuhrmann, N., Prakash, C., & Kaiser, T. S. (2023). Polygenic adaptation from standing genetic variation allows rapid ecotype formation. Elife, 12, e82824. doi:10.7554/eLife.82824.

Ghalambor, C. K., McKay, J. K., Carroll, S. P., & Reznick, D. N. (2007). Adaptive versus non-adaptive phenotypic plasticity and the potential for contemporary adaptation in new environments. Functional Ecology, 21(3), 394–407. doi:10.1111/j.1365-2435.2007.01283.x.

Gibson, G., & Dworkin, I. (2004). Uncovering cryptic genetic variation. Nature Reviews Genetics 5, 681–690. doi:10.1038/nrg1426.

Gong, L. I., & Bloom, J. D. (2014). Epistatically interacting substitutions are enriched during adaptive protein evolution. PLoS Genetics, 10(5). doi:10.1371/journal.pgen.1004328.

Griswold, C. (2006). Gene flow's effect on the genetic architecture of a local adaptation and its consequences for QTL analyses. Heredity, 96, 445-453. doi:10.1038/sj.hdy.6800822.

Hansen, T. F., Álvarez-Castro, J. M., Carter, A. J., Hermisson, J., & Wagner, G. P. (2006). Evolution of genetic architecture under directional selection. Evolution, 60(8), 1523-1536. doi:10.1111/j.0014-3820.2006.tb00498.x.

Hansen, T. F. (2013). Why epistasis is important for selection and adaptation. Evolution, 67(12), 3501–3511. doi:10.1111/evo.12214.

Hill, W. G., Goddard, M. E., & Visscher, P. M. (2008). Data and theory point to mainly additive genetic variance for complex traits. PLOS Genetics, 4(2), e1000008. doi:10.1371/journal.pgen.1000008.

Hirai, Y., & Kimura, M. T. (1997). Incipient reproductive isolation between two morphs of *Drosophila elegans* (Diptera: Drosophilidae). Biological Journal of the Linnean Society, 61(4), 501-513. doi:10.1111/j.1095-8312.1997.tb01804.x.

Huang, Y., Lack, J. B., Hoppel, G. T., & Pool, J. E. (2021). Parallel and population-specific gene regulatory evolution in cold-adapted fly populations. Genetics, 218(3). doi:10.1093/genetics/iyab077.

Huang, W., Richards, S., Carbone, M. A., Zhu, D., Anholt, R. R. H., Ayroles, J. F., Duncan, L., Jordan, K. W., Lawrence, F., Magwire, M. M., Warner, C. B., Blankenburg, K., Han, Y., Javaid, M., Jayaseelan, J., Jhangiani, S. N., Muzny, D., Ongeri, F., Perales, L., … Mackay, T. F. C. (2012). Epistasis dominates the genetic architecture of *Drosophila* quantitative traits. Proceedings of the National Academy of Sciences, 109(39), 15553–15559. doi:10.1073/pnas.1213423109.

Juenger, T. E., Sen, S., Stowe, K. A., & Simms, E. L. (2005). Epistasis and genotype-environment interaction for quantitative trait loci affecting flowering time in *Arabidopsis thaliana*. Genetica, 123, 87-105. doi:10.1007/s10709-003-2717-1.

Krishnan, S. N., Frei, E., Swain, G. P., & Wyman, R. J. (1993). Passover: a gene required for synaptic connectivity in the giant fiber system of *Drosophila*. Cell, 73(5), 967-977. doi:10.1016/0092-8674(93)90274-T.

Krupp, J. J., Yaich, L. E., Wessells, R. J., & Bodmer, R. (2005). Identification of genetic loci that interact with cut during *Drosophila* wing-margin development. Genetics, 170(4), 1775-1795. http://dx.doi.org/10.1534/genetics.105.043125.

Lack, J. B., Cardeno, C. M., Crepeau, M. W., Taylor, W., Corbett-Detig, R. B., Stevens, K. A., Langley, C. H., & Pool, J. E. (2015). The *Drosophila*

genome nexus: a population genomic resource of 623 *Drosophila melanogaster* genomes, including 197 from a single ancestral range population. Genetics, 199(4), 1229–1241. doi:10.1534/genetics.115.174664.

Lack, J. B., Monette, M. J., Johanning, E. J., Sprengelmeyer, Q. D., & Pool, J. E. (2016). Decanalization of wing development accompanied the evolution of large wings in high-altitude *Drosophila*. Proceedings of the National Academy of Sciences, 113(4), 1014–1019. doi:10.1073/pnas.1515964113.

Lande, R. 1992. Neutral theory of quantitative genetic variance in an island model with local extinction and colonization. Evolution, 46:381–389. doi:10.1111/j.1558-5646.1992.tb02046.x.

Lange, J. D., & Pool, J. E. (2016). A haplotype method detects diverse scenarios of local adaptation from genomic sequence variation. Molecular Ecology, 25(13), 3081-3100. doi:10.1111/mec.13671.

Lea, A. J., Peng, J., & Ayroles, J. F. (2022). Diverse environmental perturbations reveal the evolution and context-dependency of genetic effects on gene expression levels. Genome Research, 32(10), 1826-1839.https://www.genome.org/cgi/doi/10.1101/gr.276430.121.

Li, H. (2013). Aligning sequence reads, clone sequences and assembly contigs with BWA-MEM. arXiv:1303.3997 [q-Bio]. http://arxiv.org/abs/1303.3997.

Lollar, M. J., da Silva Ribeiro, T., Stern. D., & Pool, J. E. (2025). Quantitative trait mapping of courtship song variation between male *Drosophila melanogaster* from two allopatric populations. biorxiv, 2025-02.

López-Varea, A., Vega-Cuesta, P., Ruiz-Gómez, A., Ostalé, C. M., Molnar, C., Hevia, C. F., Martín, M., Organista, M. F., de Celis, J., Culí, J., Esteban, N., & de Celis, J. F. (2021). Genome-wide phenotypic RNAi screen in the *Drosophila* wing: Phenotypic description of functional classes. G3, 11(12), jkab349. doi:10.1093/g3journal/jkab349.

Lowry, D. B., Lovell, J. T., Zhang, L., Bonnette, J., Fay, P. A., Mitchell, R. B., Lloyd-Reilley, J., Boe, A. R., Wu, Y., Rouquette Jr, F. M., Wynia, R. L., Weng, X., Behrman, K. D., Healey, A., Barry, K., Lipzen, A., Bauer, D., Sharma, A., Jenkins, J., Schmutz, J., Fritschi, F. B., & Juenger, T. E. (2019). QTL × environment interactions underlie adaptive divergence in switchgrass across a large latitudinal gradient. Proceedings of the

National Academy of Sciences, 116(26), 12933-12941. doi:10.1073/pnas.1821543116.

Lunzer, M., Golding, G. B., & Dean, A. M. (2010). Pervasive cryptic epistasis in molecular evolution. PLoS Genetics, 6(10). doi:10.1371/journal.pgen.1001162.

Mackay, T. F. (2001). The genetic architecture of quantitative traits. Annual Review of Genetics, 35(1), 303-339. doi:10.1146/annurev.genet.35.102401.090633.

Mackay, T. F. C. (2014). Epistasis and quantitative traits: Using model organisms to study gene–gene interactions. Nature Reviews Genetics, 15(1), 22–33. doi:10.1038/nrg3627.

Malmberg, R. L., & Mauricio, R. (2005). QTL-based evidence for the role of epistasis in evolution. Genetics Research, 86(2), 89–95. doi:10.1017/S0016672305007780.

Martin, G., & Lenormand, T. (2006). The fitness effect of mutations across environments: A survey in light of fitness landscape models. Evolution, 60(12), 2413-2427. doi:10.1111/j.0014-3820.2006.tb01878.x.

Massey, J. H., & Wittkopp, P. J. (2016). The genetic basis of pigmentation differences within and between *Drosophila* species. Current Topics in developmental Biology, 119, 27-61. doi:10.1016/bs.ctdb.2016.03.004.

Mathews, K. L., Malosetti, M., Chapman, S., McIntyre, L., Reynolds, M., Shorter, R., & Van Eeuwijk, F. (2008). Multi-environment QTL mixed models for drought stress adaptation in wheat. Theoretical and Applied Genetics, 117, 1077-1091. doi:10.1007/s00122-008-0846-8.

McGuigan, K., & Sgro, C. M. (2009). Evolutionary consequences of cryptic genetic variation. Trends in Ecology & Evolution, 24(6), 305-311. doi:10.1016/j.tree.2009.02.001.

Okada, H., Ebhardt, H. A., Vonesch, S. C., Aebersold, R., & Hafen, E. (2016). Proteome-wide association studies identify biochemical modules associated with a wing-size phenotype in *Drosophila melanogaster*. Nature Communications, 7(1), 12649. http://dx.doi.org/10.1038/ncomms12649.

Orr, H. A. (1998). The population genetics of adaptation: the distribution of factors fixed during adaptive evolution. Evolution, 52(4), 935–949. doi:10.1111/j.1558-5646.1998.tb01823.x.

Orr, H. A., & Betancourt, A. J. (2001). Haldane's sieve and adaptation from the standing genetic variation. Genetics, 157(2), 875-884. doi:10.1093/genetics/157.2.875.

Papa, R., Kapan, D. D., Counterman, B. A., Maldonado, K., Lindstrom, D. P., Reed, R. D., Nijhout, H. F., Hrbek, T., & McMillan, W. O. (2013). Multi-allelic major effect genes interact with minor effect QTLs to control adaptive color pattern variation in *Heliconius erato*. PLoS One, 8(3), e57033. doi:10.1371/journal.pone.0057033.

Parker, J., & Struhl, G. (2015). Scaling the *Drosophila* wing: TOR-dependent target gene access by the Hippo pathway transducer Yorkie. PLoS Biology, 13(10), e1002274.. http://dx.doi.org/10.1371/journal.pbio.1002274.

Paul, L., Wang, S. H., Manivannan, S. N., Bonanno, L., Lewis, S., Austin, C. L., & Simcox, A. (2013). Dpp-induced Egfr signaling triggers postembryonic wing development in *Drosophila*. Proceedings of the National Academy of Sciences, 110(13), 5058-5063. http://dx.doi.org/10.1073/pnas.1217538110.

Pitchers, W., Nye, J., Márquez, E. J., Kowalski, A., Dworkin, I., & Houle, D. (2019). A multivariate genome-wide association study of wing shape in Drosophila melanogaster. Genetics, 211(4), 1429-1447. doi:10.1534/genetics.118.301342.

Pool, J. E. (2016). Genetic mapping by bulk segregant analysis in Drosophila: experimental design and simulation-based inference. Genetics, 204(3), 1295-1306. https://doi.org/10.1534/genetics.116.192484.

Pool, J. E., Braun, D. T., & Lack, J. B. (2017). Parallel evolution of cold tolerance within *Drosophila melanogaster*. Molecular Biology and Evolution, 34(2), 349–360. doi:10.1093/molbev/msw232.

Pritchard, J. K., Pickrell, J. K., & Coop, G. (2010). The genetics of human adaptation: hard sweeps, soft sweeps, and polygenic adaptation. Current Biology, 20(4), R208-R215. doi:10.1016/j.cub.2009.11.055.

Reed, L. K., Lee, K., Zhang, Z., Rashid, L., Poe, A., Hsieh, B., Deighton, N., Glassbrook, N., Bodmer, R. & Gibson, G. (2014). Systems genomics of metabolic phenotypes in wild-type *Drosophila melanogaster*. Genetics, 197(2), 781-793. doi:10.1534/genetics.114.163857.

Reynolds, J., Weir, B. S., & Cockerham, C. C. (1983). Estimation of the coancestry coefficient: basis for a short-term genetic distance. Genetics, 105(3), 767-779. doi:10.1093/genetics/105.3.767.

Rogers, W. A., Grover, S., Stringer, S. J., Parks, J., Rebeiz, M., & Williams, T. M. (2014). A survey of the trans-regulatory landscape for *Drosophila melanogaster* abdominal pigmentation. Developmental Biology, 385(2), 417-432. doi:10.1016/j.ydbio.2013.11.013.

Rutherford, S. L., & Lindquist, S. (1998). Hsp90 as a capacitor for morphological evolution. Nature, 396(6709), 336-342. doi:10.1038/24550.

Savolainen, O., Lascoux, M., & Merilä, J. (2013). Ecological genomics of local adaptation. Nature Reviews Genetics, 14, 807-820. doi:10.1038/nrg3522.

Schertel, C., Albarca, M., Rockel-Bauer, C., Kelley, N. W., Bischof, J., Hens, K., van Nimwegen, E., Basier, K., & Deplancke, B. (2015). A large-scale, in vivo transcription factor screen defines bivalent chromatin as a key property of regulatory factors mediating *Drosophila* wing development. Genome Research, 25(4), 514-523. doi:10.1101/gr.181305.114.

Schlötterer, C. (2023). How predictable is adaptation from standing genetic variation? Experimental evolution in *Drosophila* highlights the central role of redundancy and linkage disequilibrium. Philosophical Transactions of the Royal Society B, 378(1877), 20220046. doi:10.1098/rstb.2022.0046.

Ségurel, L., & Bon, C. (2017). On the evolution of lactase persistence in humans. Annual review of genomics and human genetics, 18(1), 297-319. doi:10.1146/annurev-genom-091416-035340.

Spitze, K. (1993). Population structure in *Daphnia obtusa*: quantitative genetic and allozymic variation. Genetics. 135:367–374. doi:10.1093/genetics/135.2.367

Sprengelmeyer, Q. D., Lack, J. B., Braun, D. T., Monette, M. J., & Pool, J. E. (2022). The evolution of larger size in high-altitude Drosophila melanogaster has a variable genetic architecture. G3, 12(3), jkab454. doi:10.1093/g3journal/jkab454.

Sprengelmeyer, Q. D., Mansourian, S., Lange, J. D., Matute, D. R., Cooper, B. S., Jirle, E. V., Stensmyr, M. C., & Pool, J. E. (2020). Recurrent collection of *Drosophila melanogaster* from wild African environments and

genomic insights into species history. Molecular Biology and Evolution, 37(3), 627–638. doi:10.1093/molbev/msz271.

Sprengelmeyer, Q. D., & Pool, J. E. (2021). Ethanol resistance in *Drosophila melanogaster* has increased in parallel cold-adapted populations and shows a variable genetic architecture within and between populations. Ecology and Evolution, 11(21), 15364–15376. doi:10.1002/ece3.8228.

Starr, T. N., & Thornton, J. W. (2016). Epistasis in protein evolution. Protein Science, 25(7), 1204-1218. doi:10.1002/pro.2897.

Steiner, C. C., Weber, J. N., & Hoekstra, H. E. (2007). Adaptive variation in beach mice produced by two interacting pigmentation genes. PLoS Biology, 5(9), e219. doi:10.1371/journal.pbio.0050219.

Stitzer, M. C., & Ross-Ibarra, J. (2018). Maize domestication and gene interaction. New Phytologist, 220(2), 395-408. doi:10.1111/nph.15350.

Torgeman, S., & Zamir, D. (2023). Epistatic QTLs for yield heterosis in tomato. Proceedings of the National Academy of Sciences, 120(14), e2205787119. doi:10.1073/pnas.2205787119.

Trindade, S., Sousa, A., Xavier, K. B., Dionisio, F., Ferreira, M. G., & Gordo, I. (2009). Positive epistasis drives the acquisition of multidrug resistance. PLOS Genetics, 5(7), e1000578. doi:10.1371/journal.pgen.1000578.

Van Rossum, G., & Drake, F. L. (2009). Python 3 Reference Manual. Scotts Valley, CA: CreateSpace.

Vijendravarma, R. K., & Kawecki, T. J. (2013). Epistasis and maternal effects in experimental adaptation to chronic nutritional stress in *Drosophila*. Journal of Evolutionary Biology, 26(12), 2566-2580. doi:10.1111/jeb.12248.

Whitlock, M. C., Phillips, P. C., Moore, F. B.-G., & Tonsor, S. J. (1995). Multiple fitness peaks and epistasis. Annual Review of Ecology and Systematics, 26(1), 601–629. doi:10.1146/annurev.es.26.110195.003125.

Willmer, P. G., & Unwin, D. M. (1981). Field analyses of insect heat budgets: reflectance, size and heating rates. Oecologia, 50, 250-255. doi:10.1007/BF00348047.

Wright, S. (1931). Evolution in Mendelian populations. Genetics, 16(2), 97–159. doi:10.1093%2Fgenetics%2F16.2.97.

Yeaman, S. & Otto, S. P. (2011). Establishment and maintenance of adaptive genetic divergence under migration, selection, and drift. Evolution, 65(7), 2123–2129. doi:10.1111/j.1558-5646.2011.01277.x.

Yeaman, S., & Whitlock, M. C. (2011). The genetic architecture of adaptation under migration-selection balance. Evolution, 65(7), 1897–1911. doi:10.1111/j.1558-5646.2011.01269.x.

Yukilevich, R., Lachance, J., Aoki, F., & True, J. R. (2008). Long-term adaptation of epistatic genetic networks. Evolution, 62(9), 2215-2235. doi:10.1111/j.1558-5646.2008.00445.x.

Zeng, Z. B., Kao, C. H., & Basten, C. J. (1999). Estimating the genetic architecture of quantitative traits. Genetics Research, 74(3), 279-289. doi:10.1017/S0016672399004255.

Zhang, F., Xie, D., Liang, M., & Xiong, M. (2016). Functional regression models for epistasis analysis of multiple quantitative traits. PLoS genetics, 12(4), e1005965. doi:10.1371/journal.pgen.1005965.

Zheng, Y., Liu, B., Wang, L., Lei, H., Prieto, K. D. P., & Pan, D. (2017). Homeostatic control of Hpo/MST kinase activity through autophosphorylation-dependent recruitment of the STRIPAK PP2A phosphatase complex. Cell Reports, 21(12), 3612-3623. doi:10.1016/j.celrep.2017.11.076.

Zhou, S., Campbell, T. G., Stone, E. A., Mackay, T. F., & Anholt, R. R. (2012). Phenotypic plasticity of the *Drosophila* transcriptome. PLoS genetics, 8(3), e1002593. doi:10.1371/journal.pgen.1002593.